The retreat pattern of glaciers controls the occurrence of turbidity currents on high-latitude fjord deltas

A. Normandeau[1], P. Dietrich[2], J. Hughes Clarke[3], W. Van Wychen[4], P. Lajeunesse[5], D. Burgess[6], J-F. Ghienne[7],

[1] Geological Survey of Canada (Atlantic), Natural Resources Canada, Dartmouth, Nova Scotia, B2Y 4A2, Canada

[2] Department of Geology, Auckland Park Kingsway Campus, University of Johannesburg, Johannesburg, South Africa

[3] Center for Coastal and Ocean Mapping, University of New Hampshire, 24 Colovos Road, Durham, New Hampshire 03824, USA

[4] Defense Research and Development Canada, Department of National Defense, Ottawa, Canada.

[5] Centre d’Études Nordiques & Département de Géographie, Université Laval, 2405 Rue de la Terrasse, Québec, Québec G1V 0A6, Canada

[6] Natural Resources Canada, Geological Survey of Canada, 601 Booth St., Ottawa, ON K1A 0E8, Canada

[7] Institut de Physique du Globe de Strasbourg, UMR 7516 CNRS/Université de Strasbourg, 1 rue Blessig, 67084 Strasbourg, France

Corresponding author: Alexandre Normandeau (alexandre.normandeau@canada.ca)

Key points:

- Glacial erosion is necessary to provide the sediment supply required for turbidity currents to be generated on delta fronts
- Lakes formed during glacial retreat significantly alter sediment delivery, stopping turbidity currents
- Pattern of retreating glaciers dictates the non-linear nearshore hydrodynamics of fjords

Abstract

Glacier and ice sheet mass loss as a result of climate change is driving important coastal changes in Arctic fjords. Yet, limited information exists for Arctic coasts regarding the influence of glacial erosion and ice mass loss on the occurrence and character of turbidity currents in fjords which themselves affect delta dynamics. Here, we show how glacial erosion and the production of meltwaters and sediments associated with the melting of retreating glaciers control the generation of turbidity currents in fjords of eastern Baffin Island (Canada). The subaqueous parts of 31 river mouths were mapped by high-resolution swath bathymetry along eastern Baffin Island in order to assess the presence or absence of sediment waves formed by turbidity currents on delta fronts. By extracting glaciological and hydrological watershed characteristics of these river mouths, we demonstrate that the presence and areal extent of glaciers is a key control for generating turbidity currents in fjords. However, lakes formed upstream during glacial retreat significantly alter the course of sediment routing to the deltas by forming temporary sinks, leading to the cessation of turbidity currents in the fjords. Due to the different deglaciation stages of watersheds in eastern Baffin Island, we put these results into a temporal framework of watershed deglaciation to demonstrate how the retreat pattern of glaciers, through the formation and filling of proglacial lakes, affects the activity of deltas.

1 Introduction

High-latitude coasts are particularly sensitive to a warming climate which promotes ice mass loss (Gardner et al., 2011; Zwally et al., 2011), longer open sea-ice seasons (Overeem et al., 2011; Serreze et al., 2007) and, in some regions, a relative sea-level rise (e.g., Ford et al., 2018). These environmental changes in turn drastically modify Arctic coastlines, either by increasing coastal erosion (e.g., Lantuit & Pollard, 2008), or conversely, by promoting rapid progradation of deltas due to glacial ice mass loss (e.g., Bendixen et al., 2017). Fjord-head deltas constitute the main transition zones where sediment, fossil and modern organic carbon (Galy et al., 2008; Smith et al., 2015) and contaminants (e.g., Perner et al., 2010) transit to reach deeper marine environments through river-generated density flows such as turbidity currents. Hence, rapid changes in coastal dynamics have a direct impact on these fluxes and strongly affect the nearshore environment and other associated processes in the deeper segments of the fjords, such as sediment distribution, benthos development (Syvitski et al., 1989), or the burial of organic carbon, which plays a crucial role in controlling O_2 and CO_2 concentrations (Smith et al., 2015).

Despite the importance of turbidity currents in the transfer of sediment and carbon to deeper-water ecosystems (Biscara et al., 2011), remarkably little information exists on sediment transport processes on high-latitude deltas due to a lack of high-resolution bathymetric data and in-situ monitoring. In the eastern Baffin Island region (Canada) (Fig. 1), the links between the pattern of ongoing glacial retreat (Lenaerts et al., 2013) and sediment transport to the coast provide a complete understanding of the consequences of deglaciation on sediment fluxes and partitioning in fjord systems. Therefore, the factors responsible for the presence of turbidity currents during deglaciation can be precisely identified.

The effect of deglaciation on the progradation and activity of deltas is often limited to the stratigraphic record since these processes occur over hundreds to thousands of years (Dietrich et al., 2018; Winsemann et al., 2018). Therefore, the effect of the retreat pattern of glaciers on the deltaic processes are often based on outcrop studies or from the interpretation of sediment cores. Eastern Baffin Island, like many other Arctic and Antarctic regions (e.g., Velicogna, 2009), is experiencing ongoing glacial retreat, and presents a complete range of deglaciation stages: from marine terminating glaciers to complete retreat from watersheds. These different settings allow us to understand variations in sediment supply and its effect on deltaic progradation and the occurrence of turbidity currents. These variations can then be conceptualized into a temporal framework, from fully glacierized watersheds to their complete deglaciation. The modern environments of eastern Baffin Island allow us to not only understand the factors controlling the occurrence of turbidity currents but also the effect of the retreat pattern of glaciers on deltaic activity.

Here we present the results of extensive mapping of the submarine geomorphology of 31 fjord river mouths using high-resolution (≤5 m) multibeam bathymetry data and characterize their relationship to glaciological and hydrological components of their watershed. The objectives of this study are threefold. First, the linkages between submarine sedimentary processes and the glaciological and hydrological components of watersheds allows to precise the factors controlling the occurrence of turbidity current on fjord deltas. Second, the different stages of deglaciation between watersheds allow us to build a temporal framework for the effect of the retreat pattern of glaciers on deltaic activity and the occurrence of turbidity currents. Thirdly, based on the established controls over turbidity currents occurrence, we can predict where these processes are likely to be active for the entire eastern Baffin Island fjords and speculate on future trends. Our findings have implications for the interpretation of past (Holocene and older) deglaciation sequences and for the assessment of coastal dynamics of areas affected by glacial retreat worldwide.

2 Material and methods

2.1 Datasets

This study is based on the analysis of bathymetric datasets collected on the Research Vessel (RV) Nuliajuk in 2012-2014 and the Canadian Coast Guard Ship (CCGS) Amundsen between 2006 and 2014. The multibeam bathymetric data were processed at a <5 m resolution in order to clearly visualize the presence or absence of sediment waves on delta fronts. Thirty-one deltas and river mouths were mapped in this manner along the fjords of eastern Baffin Bay (Fig. 1) (e.g., Hughes-Clarke et al., 2015).

For each delta, watersheds were created using watershed analysis tools in ArcGIS and using the Baffin Island digital elevation model (DEM; 25 m horizontal resolution) from the Canadian Digital Elevation Model (CDEM) (Fig. 2). Rivers were classified using the Strahler classification and a threshold of 100 pixel was used to define a class 1 river (Fig. 2F).

For each watershed, glaciological and hydrological characteristics were extracted using zonal statistics in ArcGIS (Fig. 2). The areas (m^2) of the watersheds were calculated along with glacial ice areas, from Randolf Glacier Inventory (Pfeffer et al., 2014), and glacial ice velocity (Van Wychen et al., 2015) ($m\ y^{-1}$). The sum of glacial ice velocity (sum of pixels) was used in this study as a proxy for glacial erosion. Pixel sizes for the ice velocity were $100 \times 100\ m^2$ and the sum of the velocity for all pixels within the watershed was calculated. The ice velocity dataset covers 99% of the Randolf Glacier Inventory dataset. Two watersheds were not fully covered by the glacial ice velocity dataset and thus, this parameter was ignored for those two watersheds. Lake area was calculated using the HydroShed Global Lake Database (Messager et al., 2016). For the 31 watersheds described in detail in this study, observation of lakes smaller than what the Global Lake Database provides were added manually. For the predictive map (see Discussion), the Global Lake Database was used without modification.

Watersheds were also created for all the lakes located within the fjord-delta watersheds and data extracted from these sub-watersheds were removed from the total watershed values, producing new adjusted watershed values that exclude lake sediment trapping (Fig. 2G).

2.2 Statistical analyses

Shapiro-Wilk normality tests and QQ normal plots were used to assess normality of distributions. Since distributions were non-normal for most of the extracted parameters, a Wilcoxon-Mann-Whitney test was used to determine if active and inactive deltas had significant differences in watershed characteristic. This non-parametric test was used to test differences between two conditions (active vs inactive deltas) and glaciological and hydrological characteristics of watersheds (presence of glacial ice, ice velocity, river classification, etc.). The test was done using the independent Wilcoxon's rank-sum test in R, which is equivalent to the Mann-Whitney test. A p-value < 0.05 indicates a statistical difference between the two distributions (active and inactive deltas). In most instances, ties in the datasets were present and thus, the values were slightly modified (using *jitter* in R) in order to compute exact p-values. An effect size was then calculated in R to estimate the size of the effect observed following Field et al. (2012).

In addition to a Wilcoxon-Mann-Whitney test, the homogeneity of variance of the active and inactive deltas glaciological and hydrological parameters were compared. Since normal distributions could not be assumed for all datasets, a Fligner-Killeen test was used instead of the more common F-test. A p-value < 0.05 indicates a significant difference in variance between the two conditions.

3 Approach: Sediment waves as indicators of deltaic activity

The main terrestrial parameter driving nearshore fjord hydrodynamics is river inflow, which controls submarine delta activity by generating turbidity currents (Syvitski, 1989; Hughes Clarke, 2016). Submarine delta activity is here viewed through the prism of subaqueous sediment wave organization. In this study, submarine delta activity is therefore defined as the presence of recurring and highly energetic turbidity currents, triggered at the delta front, and flowing downslope. These turbidity currents typically form sediment waves, the presence of which along delta slope is used to assess if a particular delta is active. In the absence of direct observations of turbidity currents, we use the absence or presence of sediment waves on delta slopes as an indicator of deltaic inactivity and activity, respectively. Sediment waves, which most of them are crescentic, are interpreted as upper-flow regime bedforms, probably cyclic steps (Cartigny et al., 2011; Hughes Clarke, 2016). Cyclic steps are sediment waves that are bounded by hydraulic jumps and that migrate upstream (Kostic et al., 2010). These types of sediment waves are known to be present on active delta slopes (Fricke et al., 2015; Clare et al., 2016; Hughes Clarke, 2016; Normandeau et al., 2016) and to be formed by high-density turbidity currents (Cartigny et al., 2011); their presence indicates active processes (e.g., Smith et al., 2005; Normandeau et al., 2014).

Repeat bathymetric surveys of three submarine deltas in Oliver Sound (northeast Baffin Island) in 2006 and 2008 and of Southwind fjord between 2013 and 2018 shows that sediment waves migrated over these two-year periods (Fig. 3). Figure 3A-G shows the morphology of two delta fronts in 2006 and 2008 along with the differences in bathymetry between the two years. These data clearly show that the sediment waves have migrated between the two years and that channel erosion occurred. These seafloor changes confirm that the presence of sediment waves indicates recurring turbidity currents, and therefore, active submarine deltas. These types of sediment waves and seafloor changes are known to be the effect of turbidity currents (Corella et al., 2014; Fricke et al., 2015; Normandeau et al., 2016; Hage et al., 2018) and cannot be attributed to oceanographic processes. The absence of sediment waves conversely indicates that the deltas are no longer active and that turbidity currents do not occur.

4 Results

4.1 Glaciological and hydrological parameters of active and inactive deltas

High-resolution multibeam bathymetric imagery available for 31 river mouths and deltas reveal 16 active and 15 inactive deltas (Fig. 1). The median percentage of glacial ice in watersheds of active deltas is 50% (Q_1=37%, Q_3= 60%) compared to 22% (Q_1=14%, Q_3= 31%) for inactive ones (Fig. 4G). In order to assess if active and inactive deltas have significantly different glaciological and hydrological settings in their watershed, a non-parametric Wilcoxon-Mann-Whitney test was used. The percentage of glacial ice in the watershed is a critical factor controlling the nearshore presence of turbidity currents in fjords ($P < 0.001, r = 0.75$) (Table 1, Fig. 4G). Watersheds devoid of glacial ice all have inactive deltas whereas watersheds with glacial ice can be active or inactive depending on past pattern of retreating glacier. Some inactive deltas have comparable percentage of glacial ice in their watershed to active ones (Fig. 4G). In order to evaluate the effectiveness of lakes in trapping sediments, lake sub-watersheds were removed from all the watersheds, which provided new adjusted watersheds (Fig. 4H) with a median percentage of glacial ice of 55% (Q_1=44%, Q_3= 61%) for active deltas and 1% (Q_1=0.1%, Q_3= 5%) for inactive ones. When excluding the sub-watersheds that flow into lakes from delta watersheds, active deltas have watersheds with significantly more glacial ice than inactive deltas ($P < 0.001, r = 0.87$) (Table 1; Fig. 4H). The percentage of glacial ice in the sub-watersheds of lakes explains the inactivity of the deltas with high percentage of glacial ice in their total watershed (Fig. 4H). Additionally, a Fligner-Killeen test shows that there is no significant difference between the variances of glacial ice in active and inactive delta watersheds when comparing their total watershed ($P = 0.58$) but that there is when comparing glacial ice in the adjusted watershed ($P = 0.03$) (Table 1). This significant difference between the variances indicates that watersheds of active deltas have higher variance of glacial ice than the inactive deltas, as expressed in Figure 4H where the percentage of glacial ice in adjusted watersheds for inactive deltas largely remains below 10%, but varies between 30-90% for active deltas. Furthermore, glacial ice velocity within adjusted watersheds (Fig. 4J), which is a proxy for glacial erosion (Overeem et al., 2017), is significantly higher in active delta watersheds than in inactive ones ($P < 0.001, r = 0.83$). Other parameters such as river classification ($P = 0.11, r = 0.29$) (Fig. 4A), which is a proxy for river discharge (Strahler, 1957), or area of watershed ($P = 0.21, r = 0.22$) (Fig. 4B), show no significant differences between the active and inactive delta watersheds (Table 1). The area of adjusted watershed becomes, however, a significant parameter ($P = 0.0036, r = 0.52$) (Fig. 4C) because, in some cases where lakes are formed near the river mouth, the watershed area is diminished by 95% when excluding lake sub-watersheds.

5 Discussion

5.1 Factors controlling the occurrence of turbidity currents

This study demonstrates the different glaciological and hydrological parameters having an effect on the occurrence of turbidity currents on fjord deltas. Recent studies have shown that the watershed area and river discharge control the type of deltas created, i.e., small gilbert type deltas or deltas with long-running channels (Gales et al., 2018). However, our results show no significant differences between small and large watersheds on the occurrence of turbidity currents. Similarly, river classification, which is used as a proxy for river discharge, does not affect the occurrence of turbidity current at river mouths, although it may affect the development of submarine channels (Gales et al., 2018). Conversely, the presence of glaciers in the watersheds exerts a significant control over the occurrence of turbidity currents, which indicates that the presence of glaciers is critical for the supply of sediment to deltas. Glacial ice area and percentage of glacial ice are both important for the occurrence of turbidity currents. The percentage of glacial ice in the watershed exerts however a slightly stronger influence, likely because it provides an estimation of the proximity of the source of sediment (i.e., glacial erosion): higher percentage of glacial ice covers a larger area of the watershed, thereby providing a source of sediment close to the delta. A closer source of sediment reduces the likelihood of sediment storage within the watershed. Conversely, small glacial ice percentage are more likely to indicate a source of glacial erosion farther upstream in the watershed, thereby increasing the likelihood of watershed sediment storage.

The differences between total and adjusted watersheds clearly show the influence of lakes on preventing the delivery of sediment to deltas. These differences are most clearly illustrated when looking at glacial ice percentage in active and inactive delta watersheds. Active deltas all contain similar percentage of glacial ice in their total and adjusted watersheds. However, although the percentage of glacial ice mostly varies between 14 and 31% in inactive delta watersheds, it drastically drops to 0-5% in the adjusted watersheds. A similar trend is observed when examining the glacial ice velocity –proxy for glacial erosion– since both parameters are linked. These values clearly show that lakes are efficient in trapping sediment and preventing the formation of turbidity currents on the fjord deltas. The proximity of the ice margin to the delta hence reduces the likelihood for sediment to encounter and then being trapped in a lake.

5.2 The retreat pattern of glaciers controls the occurrence of turbidity currents

The different deglaciation stages of the watersheds of Baffin Island allow us to better understand temporal trends in the evolution of deltas in glaciated settings and provide a conceptual model for the occurrence of turbidity currents in high-latitude environments. Some watersheds are almost fully glacierized whereas others are completely deglaciated. Examining the differences in deltaic processes and activity for this wide range of glacierized settings allows us to understand the temporal variations in sediment supply and propose a model for the evolution of a single delta/watershed during the retreat of glaciers (Fig. 5). This model begins when ice-margins become land-based and ends when ice-margins have completely retreated from the watershed.

The results presented here clearly demonstrate the critical role played by glacial erosion and the retreat pattern of glaciers across watersheds in modifying the type of sediment supply to fjords (Fig. 5). The supply of sediment from glacial erosion is assumed to remain relatively constant during glacier retreat (Fig 5A), as suggested by the presence of turbidity currents on deltas with watersheds comprising from 30% to 90% glacial ice. Glacial erosion provides large volumes of sediment when there is a direct connection between glacier and fjord-delta, which allows turbidity currents to form. However, during the retreat of the glaciers, proglacial lakes can form because of moraine damming, glacial overdeepening, isostatic flexure or structural inheritance (Carrivick & Tweed, 2013; Dietrich et al., 2017), and significantly alter the delivery of sediment to the ocean. When lakes form, sediment supply to the fjord-head delta shuts down as sediment is trapped upstream in lakes, drastically modifying the hydrodynamics of the marine nearshore environment due to severe sediment starvation (Fig. 5A, C). Both small and large lakes act the same way in trapping sediment upstream of the delta. Sediment starvation is not due to reduced sediment supply from the glaciers but is due to sediment not reaching the coast. Because of sediment starvation, some deltas appear to have been significantly eroded, forming bays while upstream lakes in the watershed are being filled with sediment (Fig. 5C). However, once sediment completely fills the lakes, which appears to have occurred in some watersheds (Fig. 5D), deltas can be reactivated on the long term since the course of the river down to the fjord is re-established (Fig. 5). Hence, although all sizes of lakes are efficient in trapping sediment, the size of lakes influences the time period during which sediment starvation on fjord deltas occurs. Finally, when glaciers retreat from the watersheds, there is no longer enough sediment supplied through glaciofluvial rivers to generate turbidity currents, which leads to the cessation of turbidity currents and the erosion of the deltas (Fig. 5A).

Recent studies have shown that delta progradation is rapid in watersheds affected by glacial ice mass loss even during relative sea-level rise (Bendixen et al., 2017), which lead us to conclude that shallow bays or shelves, in some cases formed by a drowned former delta plain and which are not prone to the formation of turbidity currents, would be quickly filled by the prograding deltas, after which turbidity currents would form in deeper environments. Therefore, the presence of a shallow bay or shelf in nearshore fjords does not preclude on the long term the formation of turbidity currents after rapid filling of the shallow nearshore environment. Possible limitations to this model nonetheless include depth of the prodelta during the transition from an inactive delta to an active one (i.e., the time it takes for deltas to fill shallow bays).

5.3 Can we predict the occurrence of turbidity currents from glaciological and hydrological watershed characteristics?

Based on the results of this study, the terrestrial glaciological and hydrological characteristics of watersheds are used to identify fjords where turbidity currents are very likely, possibly or unlikely to be presently occurring. The percentage of glacial ice within the adjusted watersheds (excluding lake sub-watersheds) proved to be the most significant parameter for the presence of turbidity currents (Table 1). Therefore, this parameter was used to predict the location of active and inactive deltas for 644 fjord deltas of eastern Baffin Island (Fig. 6) where 1) less than 10% glacial ice in adjusted watershed suggests that the deltas are inactive (unlikely in Fig. 6B); 2) between 10 and 20% glacial ice suggests that they are possibly active (possible in Fig. 6B); and 3) more than 20% glacial ice in adjusted watersheds suggest that the deltas are active (very likely in Fig. 6B). These thresholds applied to the 31 known deltas yields a 6.5% error where two inactive deltas were mistakenly interpreted as active. In these two cases, other parameters such as moraine damming or storing of sediment within the sediment-routing system appears to play a role but could not be quantified. Using percent glacial ice in adjusted watersheds is thus a strong proxy for predicting where turbidity currents occur in high-latitude fjords.

Although recent studies have suggested that glacier-derived sediment flux control the progradation of deltas (Bendixen et al., 2017; Dietrich et al., 2017), our findings reveal that the pattern of glacial retreat, i.e., the formation of lake due to moraine damming or glacial overdeepening, is more important than the simple presence/absence of a glacier in the watershed on the occurrence of turbidity currents. Of the 644 fjord delta watersheds of eastern Baffin Island, 48% likely have inactive deltas, 9% have deltas that are possibly active and 43% likely have active deltas. Although 60% of the deltas have an elevated proportion of glacial ice (>10 %) in their watersheds, only 52% possibly or likely have turbidity currents at their fronts because of the effect of lake trapping that prevents sediment delivery to the fjords. It is however important to note that this likelihood of the occurrence of turbidity currents (Fig. 6B) is only applicable in the modern configuration of lake distribution, which inherently evolve through time.

As retreat of glaciers is ongoing, the pattern of retreat may modify the future hydrological and glaciological characteristics, which will then have a direct impact on the occurrence of turbidity currents in fjords. For example, if there is a stillstand during the retreat of glaciers, it is likely to construct a frontal moraine, which will then form a moraine-damned proglacial lake that traps sediment. Conversely, if the retreat of glaciers is continuous, the formation of a proglacial lake is less likely, allowing continuous sediment delivery to fjord-deltas. Currently, studies have shown that the retreat of glaciers and ice-mass loss has accelerated in the beginning of the 21st century due to higher summer temperatures with little change in annual precipitation (Gardner et al., 2012) and that this ice mass loss appears irreversible until the end of the century (Lenaerts et al., 2013). If this accelerated ice mass loss continues as predicted, we speculate that moraine-damned lake will be less likely to form, thus enhancing in the short term the occurrence of turbidity currents in Baffin fjords. Some lakes may be filled which will allow some deltas to be reactivated. However, if ice-mass loss continues until completely melting, the occurrence of turbidity currents will cease and will have an abrupt effect on the hydrodynamics of fjords.

6 Conclusions

This study used the various stages of deglaciation of eastern Baffin Island to illustrate the role of the retreat pattern of glaciers on the activity of deltas through the occurrence of turbidity currents. We show that the supply of sediment to fjords, which is necessary for the formation of turbidity currents, is controlled by glacial erosion and hampered by the presence of lakes in the sediment-routing system. Glaciers on land are a necessary condition for the erosion of bedrock and the supply of large volumes of sediment to coastal and nearshore environments whereas lakes can prevent delivery to the fjords. These factors controlling the occurrence of turbidity currents were then conceptualized in a temporal framework since eastern Baffin Island comprises watersheds which are fully glacierized to fully deglaciated. These stages of deglaciation could thus be used to demonstrate the evolution of a retreating glacier and the formation of lakes on the non-linear activity of deltas (Fig. 5). Although this study is based on the modern environment, it can be used as a way to further our understanding of the effects of late-Pleistocene/early Holocene deglaciation on fjord sedimentation and to estimate future occurrence of turbidity currents in response to climate change.

This conceptual model is applicable to other high- to mid-latitude, high-relief (fjord) glacierized areas where glaciers feed –or not– fjord systems, such as in Arctic and Antarctic Islands, Alaska, Patagonia and New Zealand. In addition, since the formation of lakes during glacial retreat is highly variable in space and time, the timespan of delta activity is poorly predictable. Watersheds where glaciers are retreating, which is a general trend in the Arctic due to climate change (Lenaerts et al., 2013), may develop proglacial lakes in the near future, which will suddenly shut down the fjord nearshore hydrodynamics. Once lakes are filled, deltaic sedimentary processes may become active again. The acceleration of ice-mass loss however suggest that moraine-damned lakes are less likely to form in the future in the absence of glacial stillstands, potentially enhancing temporarily the occurrence of turbidity currents in Baffin fjords. Finally, following the retreat of the glaciers from the watersheds, sediment supply will abruptly drop due to cessation of glacial supply or rerouting of glacial sediments and meltwaters to adjacent basins. Future pattern of retreating glaciers will dictate the non-linear nearshore hydrodynamics of fjords and its impact on carbon burials and ecosystems and should be taken into account in models dealing with high-latitude fjord hydrodynamics.

Acknowledgements

The authors wish to thank ArcticNet for the multibeam data collection. The multibeam data collected for this study are available at http://www.omg.unb.ca/Projects/Arctic/. The extracted glaciological and hydrological data are available in the supplementary material. This study was funded by the Geological Survey of Canada.

References

Bendixen, M., Iversen, L. L., Bjørk, A. A., Elberling, B., Westergaard-Nielsen, A., Overeem, I., Barnhart, K.R., Khan, S.A. et al. (2017). Delta progradation in Greenland driven by increasing glacial mass loss. *Nature*, *550*(7674), 101.

Biscara, L., Mulder, T., Martinez, P., Baudin, F., Etcheber, H., Jouanneau, J. M., & Garlan, T. (2011). Transport of terrestrial organic matter in the Ogooué deep sea turbidite system (Gabon). *Marine and Petroleum Geology*, *28*(5), 1061-1072.

Carrivick, J. L., & Tweed, F. S. (2013). Proglacial lakes: character, behaviour and geological importance. *Quaternary Science Reviews*, *78*, 34-52.

Cartigny, M. J., Postma, G., van den Berg, J. H., & Mastbergen, D. R. (2011). A comparative study of sediment waves and cyclic steps based on geometries, internal structures and numerical modeling. *Marine Geology*, *280*(1-4), 40-56.

Clare, M. A., Clarke, J. H., Talling, P. J., Cartigny, M. J., & Pratomo, D. G. (2016). Preconditioning and triggering of offshore slope failures and turbidity currents revealed by most detailed monitoring yet at a fjord-head delta. *Earth and Planetary Science Letters*, *450*, 208-220.

Corella, J. P., Arantegui, A., Loizeau, J. L., DelSontro, T., Le Dantec, N., Stark, N., ... &

Girardclos, S. (2014). Sediment dynamics in the subaquatic channel of the Rhone delta (Lake Geneva, France/Switzerland). *Aquatic sciences*, *76*(1), 73-87.

Dietrich, P., Ghienne, J. F., Normandeau, A., & Lajeunesse, P. (2017). Reconstructing ice-margin retreat using delta morphostratigraphy. *Scientific reports*, *7*(1), 16936.

Dietrich, P., Ghienne, J. F., Lajeunesse, P., Normandeau, A., Deschamps, R., & Razin, P. (2018). Deglacial sequences and glacio-isostatic adjustment: Quaternary compared with Ordovician glaciations. *Geological Society, London, Special Publications*, *475*, SP475-9.

Field, A., Miles, J., & Field, Z. (2012). *Discovering statistics using R*. Sage publications.

Ford, J. D., Couture, N., Bell, T., & Clark, D. G. (2017). Climate change and Canada's north coast: Research trends, progress, and future directions. *Environmental Reviews*, *26*(1), 82-92.

Fricke, A. T., Sheets, B. A., Nittrouer, C. A., Allison, M. A., & Ogston, A. S. (2015). An examination of Froude-supercritical flows and cyclic steps on a subaqueous lacustrine delta, Lake Chelan, Washington, USA. *Journal of Sedimentary Research*, *85*(7), 754-767.

Gales, J. A., Talling, P. J., Cartigny, M. J., Hughes Clarke, J., Lintern, G., Stacey, C., & Clare, M. A. (2018). What controls submarine channel development and the morphology of deltas entering deep-water fjords?. *Earth Surface Processes and Landforms*.

Galy, V., France-Lanord, C., & Lartiges, B. (2008). Loading and fate of particulate organic carbon from the Himalaya to the Ganga–Brahmaputra delta. *Geochimica et Cosmochimica Acta*, *72*(7), 1767-1787.

Gardner, A., Moholdt, G., Arendt, A., & Wouters, B. (2012). Accelerated contributions of Canada's Baffin and Bylot Island glaciers to sea level rise over the past half century. *The Cryosphere*, *6*(5), 1103.

Gardner, A. S., Moholdt, G., Wouters, B., Wolken, G. J., Burgess, D. O., Sharp, M. J., ... & Labine, C. (2011). Sharply increased mass loss from glaciers and ice caps in the Canadian Arctic Archipelago. *Nature*, *473*(7347), 357.

Hage, S., Cartigny, M. J., Clare, M. A., Sumner, E. J., Vendettuoli, D., Hughes Clarke, J. E., Hubbard, S.M., Vardy, M.E. et al. (2018). How to recognize crescentic bedforms formed by supercritical turbidity currents in the geologic record: Insights from active submarine channels. *Geology*, *46*(6), 563-566.

Hughes Clarke, J. E., Muggah, J., Renoud, W., Bell, T., Forbes, D. L., Cowan, B., & Kennedy, J. (2014). Reconnaissance seabed mapping around Hall and Cumberland Peninsulas, Nunavut: Opening up southeast Baffin Island to nearshore geological investigations. *Summary of activities,* 133-144.

Hughes Clarke, J. E. (2016). First wide-angle view of channelized turbidity currents links migrating cyclic steps to flow characteristics. *Nature communications*, *7*, 11896.

Kostic, S., Sequeiros, O., Spinewine, B., & Parker, G. (2010). Cyclic steps: A phenomenon of supercritical shallow flow from the high mountains to the bottom of the ocean. *Journal of Hydro-environment Research*, *3*(4), 167-172.

Lantuit, H., & Pollard, W. H. (2008). Fifty years of coastal erosion and retrogressive thaw slump activity on Herschel Island, southern Beaufort Sea, Yukon Territory, Canada. *Geomorphology*, *95*(1-2), 84-102.

Lenaerts, J. T., van Angelen, J. H., van den Broeke, M. R., Gardner, A. S., Wouters, B., & van Meijgaard, E. (2013). Irreversible mass loss of Canadian Arctic Archipelago glaciers. *Geophysical Research Letters*, *40*(5), 870-874.

Messager, M. L., Lehner, B., Grill, G., Nedeva, I., & Schmitt, O. (2016). Estimating the volume and age of water stored in global lakes using a geo-statistical approach. *Nature communications*, *7*, 13603.

Normandeau, A., Lajeunesse, P., St-Onge, G., Bourgault, D., Drouin, S. S. O., Senneville, S., & Bélanger, S. (2014). Morphodynamics in sediment-starved inner-shelf submarine canyons (Lower St. Lawrence Estuary, Eastern Canada). *Marine Geology, 357*, 243-255.

Normandeau, A., Lajeunesse, P., Poiré, A. G., & Francus, P. (2016). Morphological expression of bedforms formed by supercritical sediment density flows on four fjord-lake deltas of the south-eastern Canadian Shield (Eastern Canada). *Sedimentology*, *63*(7), 2106-2129.

Overeem, I., Anderson, R. S., Wobus, C. W., Clow, G. D., Urban, F. E., & Matell, N. (2011). Sea ice loss enhances wave action at the Arctic coast. *Geophysical Research Letters*, *38*(17).

Overeem, I., Hudson, B. D., Syvitski, J. P., Mikkelsen, A. B., Hasholt, B., van den Broeke, M. R., ... & Morlighem, M. (2017). Substantial export of suspended sediment to the global oceans from glacial erosion in Greenland. *Nature Geoscience*, *10*(11), ngeo3046.

Perner, K., Leipe, T., Dellwig, O., Kuijpers, A., Mikkelsen, N., Andersen, T. J., & Harff, J. (2010). Contamination of arctic Fjord sediments by Pb–Zn mining at Maarmorilik in central West Greenland. *Marine pollution bulletin*, *60*(7), 1065-1073.

Pfeffer, W. T., Arendt, A. A., Bliss, A., Bolch, T., Cogley, J. G., Gardner, A. S., Hagen, J.O., Hock, R. et al. (2014). The Randolph Glacier Inventory: a globally complete inventory of glaciers. *Journal of Glaciology*, *60*(221), 537-552.

Serreze, M. C., Holland, M. M., & Stroeve, J. (2007). Perspectives on the Arctic's shrinking sea-ice cover. *science*, *315*(5818), 1533-1536.

Smith, D. P., Ruiz, G., Kvitek, R., & Iampietro, P. J. (2005). Semiannual patterns of erosion and deposition in upper Monterey Canyon from serial multibeam bathymetry. *GSA Bulletin*, *117*(9-10), 1123-1133.

Smith, R. W., Bianchi, T. S., Allison, M., Savage, C., & Galy, V. (2015). High rates of organic carbon burial in fjord sediments globally. *Nature Geoscience*, *8*(6), ngeo2421.

Strahler, A. N. (1957). Quantitative analysis of watershed geomorphology. *Eos, Transactions American Geophysical Union*, *38*(6), 913-920.

Syvitski, J. P. (1989). On the deposition of sediment within glacier-influenced fjords: oceanographic controls. *Marine Geology*, *85*(2-4), 301-329.

Syvitski, J. P., Farrow, G. E., Atkinson, R. J. A., Moore, P. G., & Andrews, J. T. (1989). Baffin Island fjord macrobenthos: bottom communities and environmental significance. *Arctic*, 232-247.

Velicogna, I. (2009). Increasing rates of ice mass loss from the Greenland and Antarctic ice sheets revealed by GRACE. *Geophysical Research Letters*, *36*(19).

Winsemann, J., Lang, J., Polom, U., Loewer, M., Igel, J., Pollok, L., & Brandes, C. (2018). Ice-marginal forced regressive deltas in glacial lake basins: geomorphology, facies variability and large-scale depositional architecture. *Boreas*.

Van Wychen, W., Copland, L., Burgess, D. O., Gray, L., & Schaffer, N. (2015). Glacier velocities and dynamic discharge from the ice masses of Baffin Island and Bylot Island, Nunavut, Canada. *Canadian Journal of Earth Sciences*, *52*(11), 980-989.

Zwally, H. J., Li, J., Brenner, A. C., Beckley, M., Cornejo, H. G., DiMARZIO, J., ... & Yi, D. (2011). Greenland ice sheet mass balance: distribution of increased mass loss with climate warming; 2003–07 versus 1992–2002. *Journal of Glaciology*, *57*(201), 88-102.

TABLE AND FIGURE CAPTIONS

Table 1: Factors controlling the presence of turbidity currents on fjord-deltas. A Wilcoxon-Mann-Whitney test was used to compare active vs inactive deltas. Percentage of glacial ice is the main controlling factor and statistical significance increases when taking lakes as efficient sediment traps into consideration (adjusted watersheds). The Fligner-Killeen test checks for homogeneity of variance between the distributions and indicates if the difference in variance is significant ($p < 0.05$) or not.

Figure 1: Distribution of the active and inactive delta watersheds along eastern Baffin Island with bathymetric examples of inactive (A, B) and active deltas (C, D, E).

Figure 2: Method for the extraction of glaciological and hydrological data: A) Satellite image of the Pangnirtung fjord-head delta and watershed; B) Delimitation of its watershed (green line); C) Extraction of glacial ice area within the watershed; D) Extraction of glacial ice velocity within the watershed; E) Extraction of the area of lakes within the watershed; F) Extraction of river classification within the watershed; G) Delimitation of the adjusted watersheds from which the previous glaciological and hydrological characteristics were re-extracted.

Figure 3: Examples of recurring turbidity currents leading to the migration of sediment waves (cyclic steps) on two fjord-head deltas between 2006 and 2008. A) Location of Oliver Sound and the fjord-head deltas; B) Bathymetry of western Oliver Sound delta in 2006; C) Bathymetry of western Oliver Sound delta in 2008; D) Elevation difference map of western Oliver Sound between 2006 and 2008 illustrating channel erosion and the migration of sediment waves; E) Bathymetry of eastern Oliver Sound delta in 2006; C) Bathymetry of eastern Oliver Sound delta in 2008; D) Elevation difference map of eastern Oliver Sound between 2006 and 2008 illustrating channel erosion and the migration of sediment waves.

Figure 4: Boxplots of the glaciological and hydrological parameters controlling turbidity currents (TC) in fjord-head deltas. River classification (A), area of watershed (B), area of adjusted watershed (C), glacial ice area (D), glacial ice area in adjusted watershed (E), percentage of lake (F), percentage of glacial ice (G), percentage of glacial ice in adjusted watershed (H), glacial ice velocity (I) and glacial ice velocity in adjusted watershed (J) were all tested against the presence or absence of sediment waves (TC or No TC). The percentage

of glacial ice in adjusted watershed (H) was found to be the main controlling factor on the presence of sediment waves and therefore, on the occurrence of turbidity currents in fjords.

Figure 5: Effect of watershed characteristics on deltaic activity. A) Proposed model for the occurrence of turbidity currents during glacier retreat: 1) A direct connection between glacial erosion and the delta will lead to the occurrence of turbidity currents (B, E). 2) The presence of a lake caused by glacial retreat (e.g., by moraine damming or glacial overdeepening) will alter the delivery of sediment to the delta (C, F). 3) However, if the lake is filled, the connection will be re-established, leading to the reactivation of turbidity currents (D, G).

Figure 6: A) Distribution of glacial ice and glacial ice velocity in eastern Baffin Island. B) Predictive map of fjord deltas with currently occurring turbidity currents. Very likely active turbidity currents have >20% glacial ice in their adjusted watersheds (excluding lake sub-watershed). Possibly active deltas (possible in B) have 10-20% glacial ice in their adjusted watersheds. Inactive deltas (unlikely in B) have less than 10% glacial ice in their adjusted watersheds.

Table 1

Variable	Wilcoxon-Mann-Whitney p-value	Effect size (r)	Fligner-Killeen p-value
Percentage glacial ice in adjusted watershed	0.000001	0.87	0.03
Sum of glacial ice velocity in adjusted watershed	0.000007	0.83	0.001
Glacial ice area in adjusted watershed	0.00001	0.79	0.0004
Percentage glacial ice in watershed	0.00003	0.75	0.58
Area of adjusted watershed	0.0036	0.52	0.003
Sum of glacial ice velocity in watershed	0.004	0.53	0.04
Glacial ice area in watershed	0.005	0.5	0.01
Percentage lake area in watershed	0.006	0.46	0.046
River classification (Strahler)	0.11	0.29	0.53
Area of watershed	0.21	0.22	0.14

Figure 1

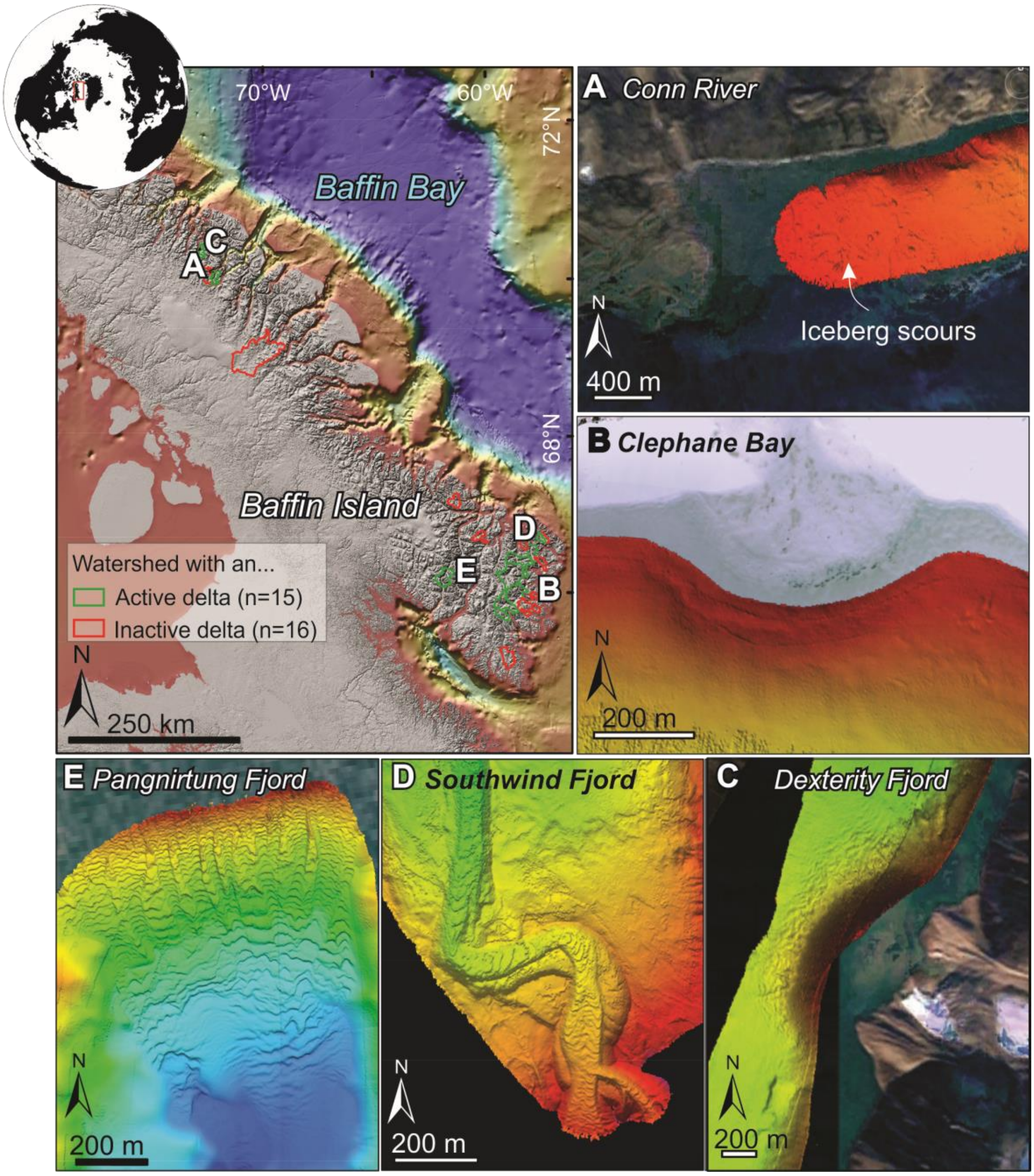
70°W
60°W
72°N
68°N
Baffin Bay
Baffin Island
A
B
C
D
E
Watershed with an...
🟩 Active delta (n=15)
🟥 Inactive delta (n=16)
N
250 km
A Conn River
Iceberg scours
N
400 m
B Clephane Bay
N
200 m
E Pangnirtung Fjord
N
200 m
D Southwind Fjord
N
200 m
C Dexterity Fjord
N
200 m

Figure 2

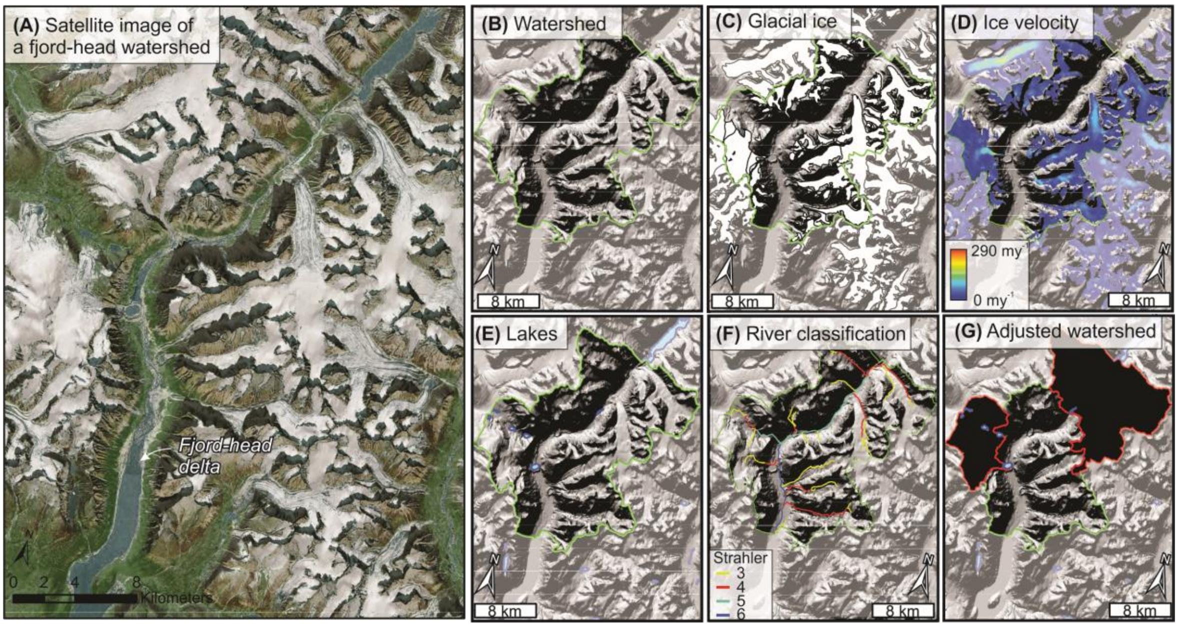
(A) Satellite image of a fjord-head watershed
Fjord-head delta
0 2 4 8 Kilometers
(B) Watershed
(C) Glacial ice
(D) Ice velocity
290 my-1
0 my-1
(E) Lakes
(F) River classification
Strahler
3
4
5
6
(G) Adjusted watershed
8 km
N

Figure 3

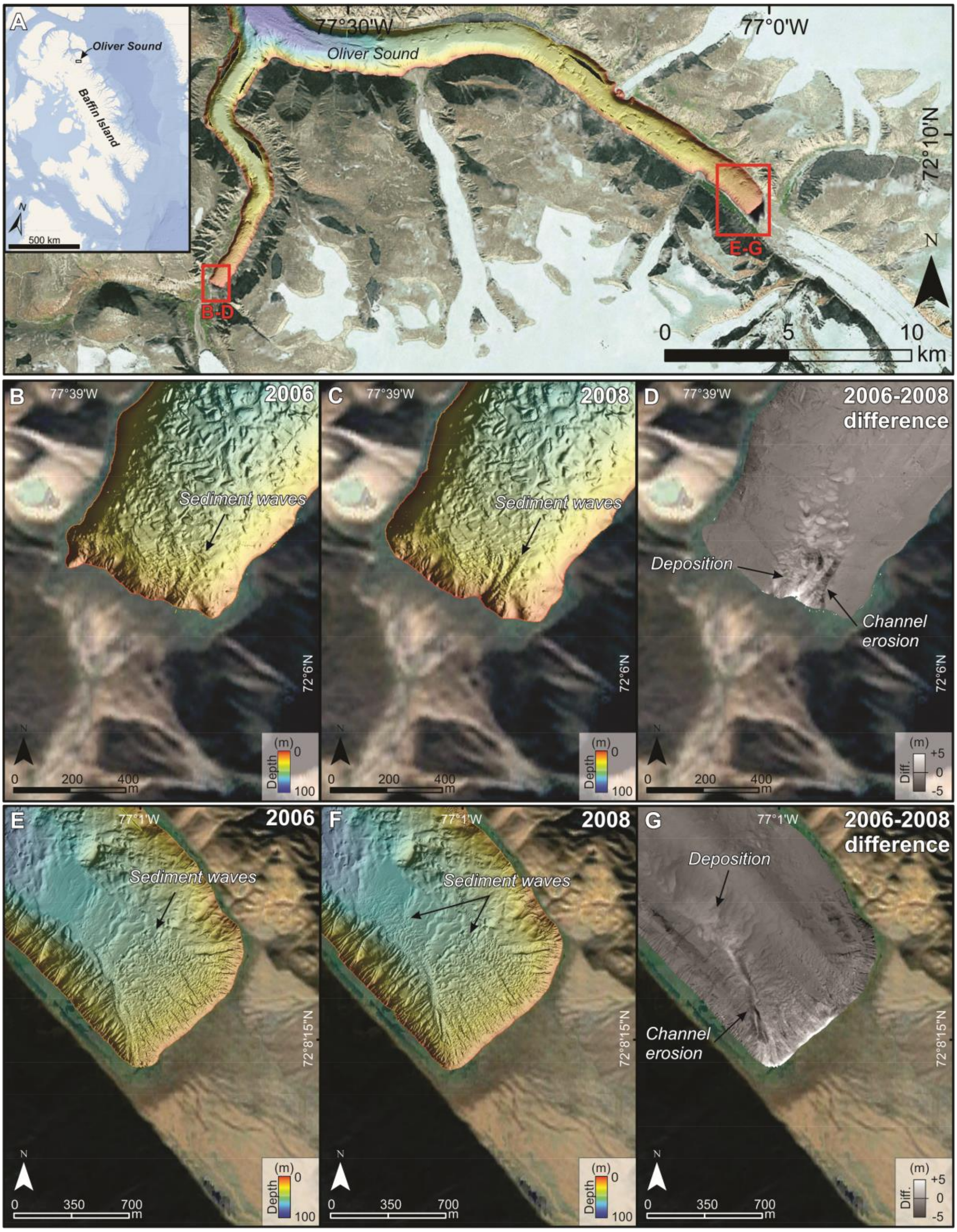
A
Oliver Sound
Baffin Island
N
500 km
77°30'W
77°0'W
Oliver Sound
72°10'N
B-D
E-G
N
0
5
10
km
B
77°39'W
2006
Sediment waves
72°6'N
N
0
200
400
m
(m)
Depth
0
100
C
77°39'W
2008
Sediment waves
72°6'N
D
77°39'W
2006-2008 difference
Deposition
Channel erosion
72°6'N
Diff.
+5
0
-5
E
77°1'W
2006
Sediment waves
72°8'15"N
350
700
F
77°1'W
2008
Sediment waves
72°8'15"N
G
77°1'W
2006-2008 difference
Deposition
Channel erosion
72°8'15"N

Figure 4

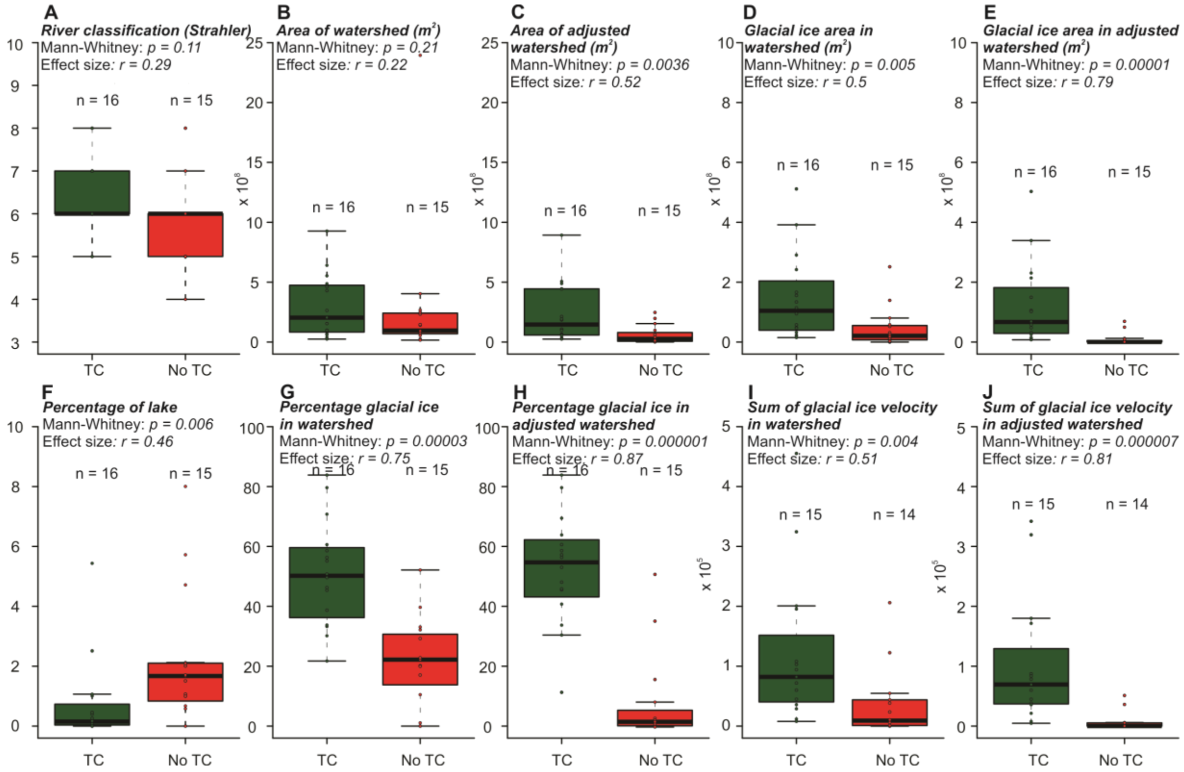
A
River classification (Strahler)
Mann-Whitney: p = 0.11
Effect size: r = 0.29
n = 16
n = 15
10
9
8
7
6
5
4
3
TC
No TC
B
Area of watershed (m²)
Mann-Whitney: p = 0.21
Effect size: r = 0.22
n = 16
n = 15
x 10⁸
25
20
15
10
5
0
TC
No TC
C
Area of adjusted watershed (m²)
Mann-Whitney: p = 0.0036
Effect size: r = 0.52
n = 16
n = 15
x 10⁸
25
20
15
10
5
0
TC
No TC
D
Glacial ice area in watershed (m²)
Mann-Whitney: p = 0.005
Effect size: r = 0.5
n = 16
n = 15
x 10⁸
10
8
6
4
2
0
TC
No TC
E
Glacial ice area in adjusted watershed (m²)
Mann-Whitney: p = 0.00001
Effect size: r = 0.79
n = 16
n = 15
x 10⁸
10
8
6
4
2
0
TC
No TC
F
Percentage of lake
Mann-Whitney: p = 0.006
Effect size: r = 0.46
n = 16
n = 15
10
8
6
4
2
0
TC
No TC
G
Percentage glacial ice in watershed
Mann-Whitney: p = 0.00003
Effect size: r = 0.75
n = 16
n = 15
100
80
60
40
20
0
TC
No TC
H
Percentage glacial ice in adjusted watershed
Mann-Whitney: p = 0.000001
Effect size: r = 0.87
n = 16
n = 15
100
80
60
40
20
0
TC
No TC
I
Sum of glacial ice velocity in watershed
Mann-Whitney: p = 0.004
Effect size: r = 0.51
n = 15
n = 14
x 10⁵
5
4
3
2
1
0
TC
No TC
J
Sum of glacial ice velocity in adjusted watershed
Mann-Whitney: p = 0.000007
Effect size: r = 0.81
n = 15
n = 14
x 10⁵
5
4
3
2
1
0
TC
No TC

Figure 5

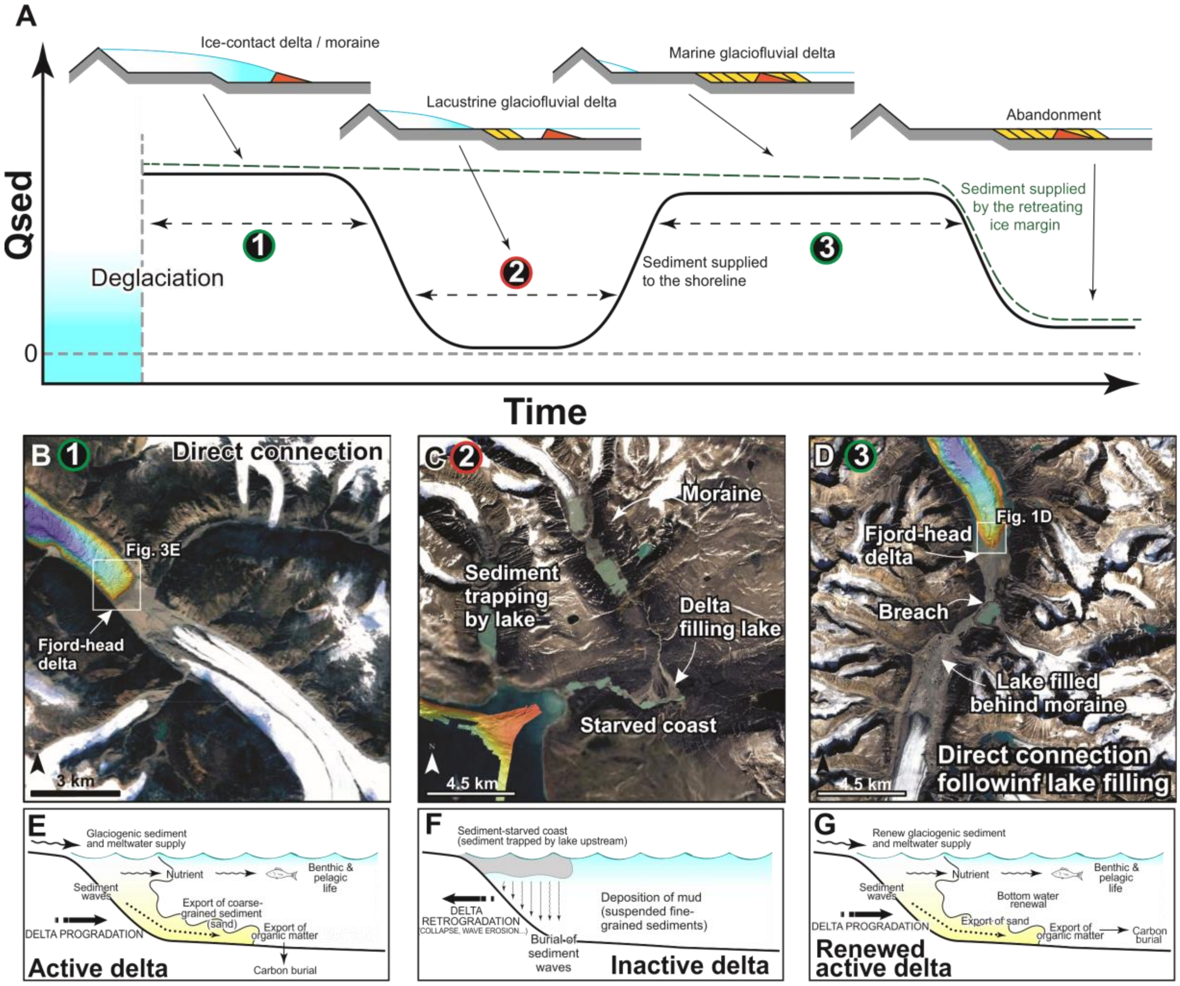
A
Qsed
0
Time
Deglaciation
Ice-contact delta / moraine
Lacustrine glaciofluvial delta
Marine glaciofluvial delta
Abandonment
1
2
3
Sediment supplied to the shoreline
Sediment supplied by the retreating ice margin
B 1
Direct connection
Fig. 3E
Fjord-head delta
3 km
C 2
Moraine
Sediment trapping by lake
Delta filling lake
Starved coast
N
4.5 km
D 3
Fig. 1D
Fjord-head delta
Breach
Lake filled behind moraine
Direct connection followinf lake filling
4.5 km
E
Glaciogenic sediment and meltwater supply
Nutrient
Benthic & pelagic life
Sediment waves
Export of coarse-grained sediment (sand)
Export of organic matter
DELTA PROGRADATION
Carbon burial
Active delta
F
Sediment-starved coast (sediment trapped by lake upstream)
DELTA RETROGRADATION
(COLLAPSE, WAVE EROSION...)
Deposition of mud (suspended fine-grained sediments)
Burial of sediment waves
Inactive delta
G
Renew glaciogenic sediment and meltwater supply
Nutrient
Benthic & pelagic life
Sediment waves
Bottom water renewal
Export of sand
Export of organic matter
Carbon burial
DELTA PROGRADATION
Renewed active delta

Figure 6

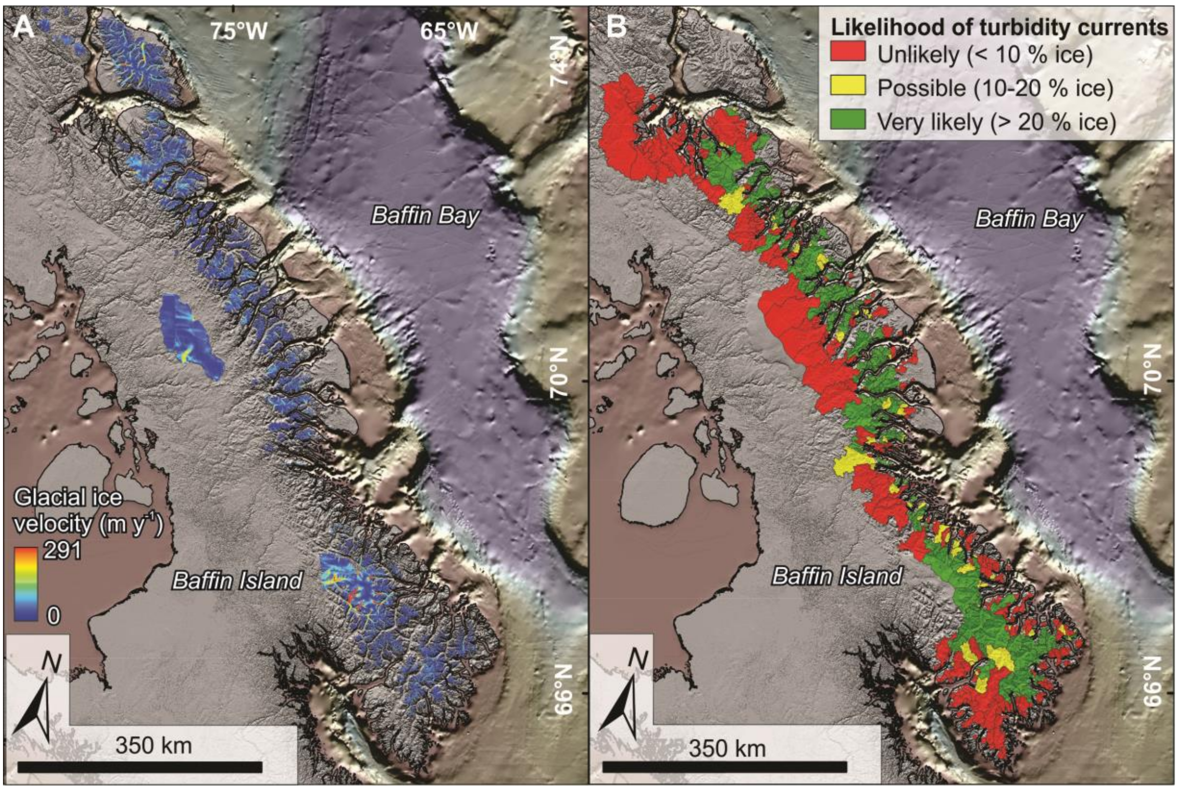
A
75°W
65°W
74°N
70°N
66°N
Baffin Bay
Baffin Island
Glacial ice velocity (m y⁻¹)
291
0
N
350 km
B
Likelihood of turbidity currents
Unlikely (< 10 % ice)
Possible (10-20 % ice)
Very likely (> 20 % ice)
Baffin Bay
Baffin Island
70°N
66°N
N
350 km